

Digital Procedures for Pattern Recognition of Diesel Spray Characteristics

A.Cavaliere, L.Tognotti, S.Pintus, R.Ragucci* and S.Zanelli

*Dipartimento di Ingegneria Chimica
Chimica Industriale e Scienza dei Materiali
Università di Pisa
Via Diotisalvi 2
58100 Pisa
Italy
* IRC-CNR, Napoli*

ABSTRACT

The paper is focused on the methodological aspects of different categories of numerical procedures to be used in data elaboration of digital images. In fact the common feature of digital imaging makes similar many techniques, which use different characteristics of interaction of light with matter and different optical set-up. A first category is the background rejecting, on which an example of application of the procedures is shown. Other categories deal with different representation of single images or part of images and their statistical elaboration or diagrams of morphological descriptors of images sequences. Example are reported

INTRODUCTION

The optical diagnostics in diesel combustion processes have been developed parallelly for two kinds of experimental devices, namely diesel engines and high pressure chambers in quiescent or flowing regimes. The differences in terms of optical accessibility and of complexity of fluid dynamic patterns in the two cases have "conditioned" also the features of the diagnostics. In the first devices, due to higher level of difficulties, the techniques are based on qualitative signatures taken on large length scales rather than on specific quantitative measurements in narrower parts of the diesel spray with high spatial resolution. For instance cinematography of emission, Shlieren or shadow patterns have been used for diesel spray characterizations in isothermal and burning conditions, whereas elastic scattering patterns have been used preferentially in "simpler" environment.

This general consideration can not be enforceable in all specific investigations and there are techniques which have been used in both environments; this is the case for single point

measurements like laser doppler anemometry. It is evident that the present trend is to make applicable inside diesel engines also the most over refined techniques, so that the limit between the two categories is not well defined and it will change in future. There is one peculiar field in which parts of the measurement methodologies are common to both categories; it concerns the pattern recognition of images taken from diesel environments. The reason of this unification is due to the fact that the images can be obtained, in both cases under the format of numerical matrices which can be elaborated with the same numerical codes. In fact, even though the images are recorded on film plates, they can be digitized with particular devices, which will be described in the following section and consequently are compatible with data processing of images digitized directly from videosegments.

Even though the data format is equal, there are still differences between the two types of visualization. In the first case the film plates can ensure very high dynamic range on the recorded intensity levels and very small physical support of the smallest sensitive element (the grain size), but they are limited in terms of repeatability and of difficulties in calibrated linearization on the intensity scales.

In the second case the use of video recording systems, like CCD and CID cameras, overcomes the aforementioned shortcomings, but the ratio between the sizes of their smallest picture elements (pixels) and the whole sensitive area is in the order of $10^{-2} - 10^{-3}$, which is very much lower than $10^{-6} - 10^{-7}$, values commonly achievable with photographic systems.

The very high information density of the film image is lost in the digitization process and it becomes comparable to the video-image (same order of pixels and sensitivity range), but it is still an advantage since it represents an information field which can be "sampled" with different spatial resolutions and different ranges of grey levels. A part from these fundamental differences,

all the images taken with any kind of detecting systems and relative to any kind of measurement (elastic or anelastic scattering, extinction, etc.) share the same problem of rejecting the background which is generated by straylight from different parts of the diesel spray and/or from the confinement walls.

This problem becomes more pressing passing from high pressure chamber to engines because of the higher level of confinement and the constraints on optical accessibility so that its solution is a crucial step on the exploitation of sophisticated two-dimensional techniques in real engines. In fact only images, "purged" of the background, where the intensity level is linked to the useful part of signals, can be further processed for their direct or statistical analysis. The main stress of the paper is posed on the digital procedures for this type of image processing. It can be considered quite a general approach, which can be followed along the guidelines of the examples reported as auxiliary help for the understanding of the procedures. These examples are also briefly described in terms of implications related to the combustion process.

The "clean" images can be subsequently used for automatic elaborations, which can be the same than those ones used in the past in diesel spray analysis (e.g. spray tip positions etc.), obtained with traditional measuring techniques or which can be obtained only taking advantage of numerical nature of the images and therefore are relatively new. Also for these elaborations, selected examples are given either for images taken inside engine combustion chambers or in nearly quiescent diesel-like conditions. Finally it is important to evidence that the features of the optical diagnostics used in the detection of images are not dealt in this paper, so that readers interested in these aspects are addressed to references quoted in bibliography.

THE IMAGE PROCESSING SYSTEM

Herein, the image processing system developed at University of Pisa with the collaboration of Istituto Elaborazione dell'Informazione, IEI CNR in Pisa (1), is briefly described: it represents an example from which the typical features of the architecture of an image processing system can be ascertained.

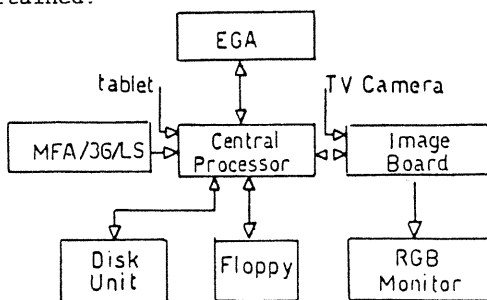


Figure 1

The hardware architecture of the work station is shown in Fig. 1. Main components are:

- a film scanner, MFA/36/LS;
- a Central Processor Unit, with 1 MB memory, 12 MHz clock and MS-DOS operating system;
- a mass memory, composed of a high density floppy disk unit and a 40 MB hard disk unit;
- an image board, which drives an RGB monitor.

It is worthwhile to give some details about the film scanner, since it generates the numerical matrix to be further elaborated, as already pointed out in the introduction.

The film scanner has been designed according to its Modular Transfer Function response (1).

A schematic representation of the scanner is shown in Fig.2. The film to be digitized is illuminated by a linear light source and the luminous flux transmitted by the transparency is focalized by an objective on a 1024 element optoelectronic array; in this way, an image of the stripe-shape region of the photogram, aligned to the Z axis of the figure, is formed on the front surface of the transducer, the dimensions of the stripe depending on distances X_0 and X_1 along the optical axis X. Scanning along Z axis is performed electronically by the transducer circuitry; scanning along Y axis is done by means of a step motor which translates the film in the Y direction. The magnification M of the objective depends on the values of the distances of X_1 and X_0 . Two values of M are selectable: with $M = 0.64$, pixels on the photograms are $24 \mu\text{m}$ wide, and the scanning area is $24 \text{ mm} \times 36 \text{ mm}$, while with $M = 1.28$, pixel dimensions are $12 \mu\text{m} \times 12 \mu\text{m}$ and the scanning area is $12 \text{ mm} \times 36 \text{ mm}$.

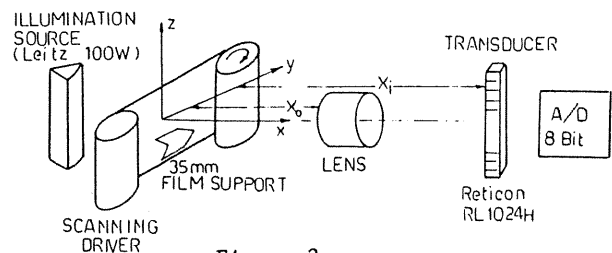


Figure 2

The video signal produced by the optoelectronic transducer is linearly quantized on 256 levels by means of an 8 bits Analog to Digital converter, over a 2.5 decades range; by setting the objective iris, this range can be shifted along an overall range of 3 decades. The software control of the scanner processes input row data in order to correct the nonuniformity of the transfer characteristics of the array elements, the nonuniformity of the light flux emitted by the luminous source and the vignetting produced by the objective; the film scanner can thus measure optical transparency of optical density with a 256 level resolution, and 3% accuracy in 3 decades range. The work station so contains a

1024 x 1024 x 8 bits image memory; the memory is loaded with input or processed data, which are displayed on a 625 line/frame TV monitor by means of 512 x 512 pixel windows.

GENERAL PURPOSE PROCEDURES FOR IMAGE PROCESSING

A general purpose software for image processing should be composed by the following part:

- a high level man-machine interface, MMI, which handles communication between the user and the system;
- a data base for images, graphs and alphanumeric data;
- a set of processing modules and thematic procedures.

In the software developed by IEI of Pisa, the MMI is composed of semantic tables which allow the user to select the operations to be executed: MMI tables are organized in a tree-like structure and the user can access operations in a transparent mode by sailing along this structure.

The set of programs is subdivided into homogeneous environments which groups function data and image handling or processing. The tree-like structure is shown in Fig. 3.

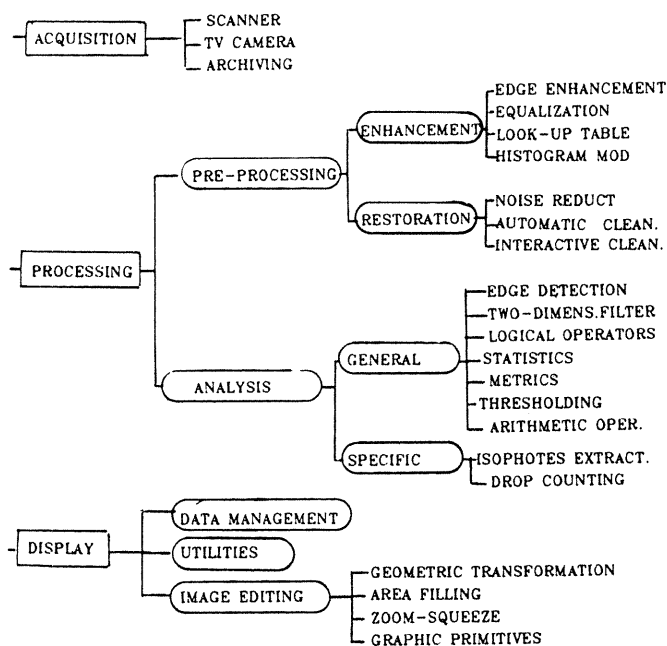


Figure 3

The user can select the following main environments:

Acquisition procedures: for images in raster format by means of the image scanner or a TV camera, or in a vector format by means of a tablet.

Processing procedures, including: preprocessing modules for geometric transform, photometric or radiometric corrections and noise reduction, as well as analysis modules, which execute mathematics or logic operation, segmentation and classification, for general and specific purposes (1) (2).

Display and utilities procedures, including data management, general purpose utility routines (file copy, print, format, etc.) and image editing.

The system has been recently used in the analysis of spray photographs (1) (2) (3).

PROCEDURES FOR BACKGROUND REJECTING

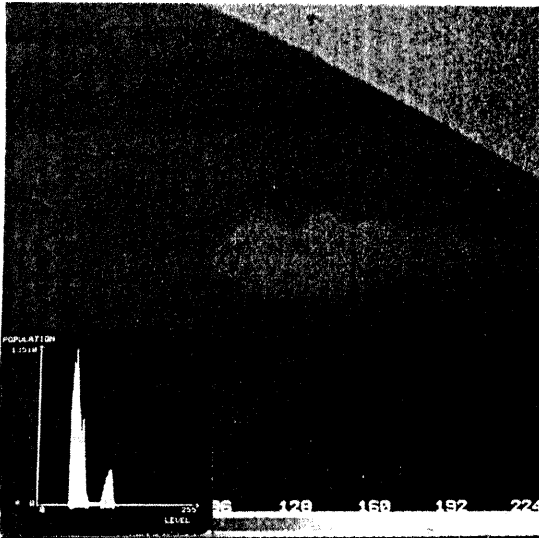
As already pointed out, digital images coming from any kind of measurement in any kind of detecting system, present the problem of rejecting the background that is generated by straylight. In this paragraph results are presented relative to a diesel spray obtained in a diesel engine (2). However, the procedures described here are of general use and they can be employed on any kind of digital image.

Figure 4a shows a typical picture (negative plate) of the diesel spray obtained as described in the previous section. It can be noted that a background luminosity is spread over the whole image and it is difficult to distinguish by simple visual observation which is the intensity level of the signal as well as which light intensity gradient is present inside the spray. Also the histogram of the intensity level population reported in Fig. 4b does not help in doing this discrimination, since it is not possible "a priori" to know whether one of the two separated like-gaussian profiles is completely attributable to the signal or to the noise. In order to abstract semi-quantitative information from this kind of pictures, different procedures have to be used:

- i) histogram modification,
- ii) thresholding,
- iii) spacial "purgin",
- iv) binarization and area filling,
- v) logical "and" between original image and binarized image or v) spray area computation.

The first operation improves the quality of the image through a linear histogram modification which extends the dynamic range of the intensity. The result of the operation is reported in Fig. 4c and 4d: the modified image and the relative population histogram can be used in the evaluation of the characteristics of the spray image in term of intensity levels. In fact the background present in Fig. 4c is clearly separated respect to the spray contours and the population histogram of Fig. 4d covers the whole available intensity range. The procedure of histogram modification is completely automatic, when the modification function has been chosen.

The operation of thresholding concerns the determination of the "threshold" interval of gray level in which the information is contained. For this purpose a false-colour scale is determined in such a way that it fills the contours of the spray. Figure 4e reports the image obtained by



Figures 4a and 4b



Figures 4c and 4d

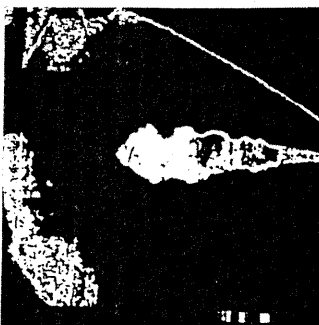


Figure 4e

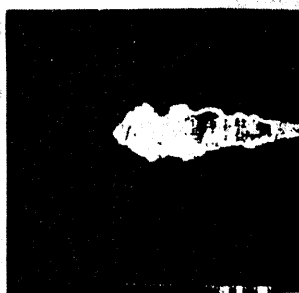


Figure 4f

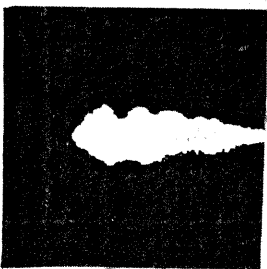


Figure 4g



Figure 4h

means of slipping a narrow look-up table (1) over a black background. It is evident that it is possible to separate in the space the spray picture from the background intensity.

It is easy on the image of Fig. 4e to reject all the intensities recorded in this spatial field which is not relevant for the pattern analysis. This procedure is the spacial "purging": only the useful part of the image is saved by the interactive action of the operator. It is important note that the operations of thresholding and purging cannot be performed automatically, even though the operator experience can be very limited and the personal bias generates a very low uncertainty (as it was evident by the fact that two different operators obtained independently very similar final image elaborations) (Fig.4d).

Finally the binarization of the image is performed attributing the highest intensity value [255] to all the pixels with intensity level inside the threshold interval. When the image presents black "holes" inside the spray zone, the area filling procedure is employed, which allows to fill the holes. The result of the last two procedures is reported in Fig. 4g. This image is ready to be analyzed in term of spray area, by computing the number of pixels contained inside the white zone (procedure v).

Further development is offered by the image so obtained: it is possible to recover the original information, in terms of gray levels, contained only in the spray zone (procedure v). This is performed through a logical "and" between the final image, showed in Fig.4g and the original one (Fig. 4a), the result being the image as Fig.4h. This procedure has been used in the qualitative analysis of the structure of diesel sprays (2)

PROCEDURES FOR IMAGE ANALYSIS. SELECTED EXAMPLES

The images obtained after the processing procedures described in the previous section can be elaborated in terms of "integral" descriptors. They are different according to the analysis which is pursued. Therefore the examples, reported in this section, are only indicative of a wider category of numerical codes (Fig. 3).

The first example concerns the measurements of the spray tip position and of the geometrical area of the longitudinal cross section of the spray. The numerical code in this case is very simple. In fact the number of the "high-value" pixels in the binarized image is directly proportional to the spray area and the coordinates of the spray contour which crosses the geometrical axis of the spray can also easily computed.

A crude approximation of the spray angle can also be obtained by these two evaluations, computing the base of the equivalent-area triangle with the same area of the spray cross section and with the same altitude than the tip penetration.

Eventually the spray angle, computed in such a way, can also be compared with the spray aperture evaluated as the angle between two tangents to the spray contours (individuated on recognizable features (1)), which pass through the nozzle center. An example of the first two elaborations (penetration and surface area) is given in Fig.5 as function of the crank angle for the same diesel engine conditions reported in reference (1).

The spray tip penetration is a nearly linear function of the crank angle with a slight "bending" of the interpolating curve in correspondence of a jet penetration $L/R = 0.7$. The decrease of the slope of the curve is usually attributed to the droplet deceleration, which is very effective only when the atomization is progressed up such a level that the aerodynamic drag on very small droplets is higher than inertial forces.

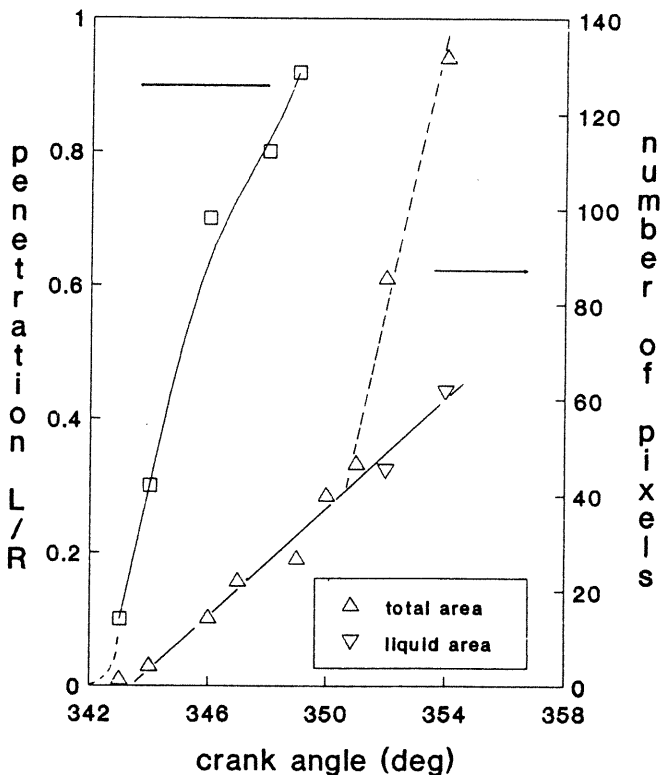


Figure 5

The area of the spray cross section is reported in terms of number of pixels. It has been evaluated on the whole sections (reported with the symbol Δ) and for two images taken at crank angle 352 and 354 it has been also evaluated the number of pixels attributable only to the part of the spray formed of liquid droplets (symbol ∇). The attribution is performed by means of a threshold technique similar to that described in the previous section and it is relatively subjective since an intensity level is chosen on the ground of interactive observation. In any case, whatsoever distinguishing between the two phases, it is clearly from Fig. 5 that the spray cross-section area increases very steeply for crank angles higher than 350. It is of interest to evidence

that nearly at the same time the spray has impinged on the chamber wall ($L/R = 1$). The discussion related to the aerodynamic pattern, which can generate the simultaneous occurrence between jet impingement and enlargement of "spray" cross section is reported in the reference (1).

Another example of digital imaging processing related to different experimental conditions is presented in the followings in order to show other potentials of digital elaborations. It refers to injections through a single-hole sac-type ($\phi = 0.25$ mm) nozzle into nearly-quiet high-pressure (1.5 MPa) environment. 40 mm^3 of fuel are injected in 3.5 msec with peak pressure of 140 MPa for two environmental temperature conditions fixed at 300 K and 800 K. The images reported in Fig.6 are the records on an intensified CCD camera of laser light scattered from droplets which cross at fixed time delay (measured from the needle lift) laser sheet with thickness of $200 \mu\text{m}$. The scattering intensities depend on the square of the droplet diameter (5), so that the intensities level in the image represent the liquid surface area of the spray cross section.

Each pattern of Fig.6 consists of four isocontours which are drawn in correspondence of 0.2, 0.4, 0.6 and 0.8 values, which refer to an arbitrary-units scale common to all patterns. The external isocontour is always correspondent to a value of 0.2, the most internal one corresponds to a value of 0.8 and it is the boundary of the black regions. The values of 0.4 and 0.6 are relative to isocontours, which are inside the former two and are located in such a way that, moving from the periphery toward the central regions, 0.2, 0.4, 0.6, 0.8 values are met. Complete specification of the optical set-up, of the scattering characteristics, and of the experimental conditions are given in the references (4), whereas in this framework Fig. 6 is commented only in relation to possible statistical elaborations. It shows on the left side an ensemble of scattering patterns taken into low temperature (300 K) environment and on the right side the images taken at the same time delays into high temperature (800 K) ambience; all patterns are relative to a spray cross section 14 mm from the nozzle outlet, when no emission could be detected, so that they are representative of spray in isothermal conditions. The sequence at low temperature shows that high levels of the fuel surface area are randomly distributed inside the whole section. In fact the black regions cover large parts of the pattern at time delay $\Delta t = 0.2, 0.5$ and 0.8 msec, whereas they are confined in narrow spots at $\Delta t = 2.4, 2.8$ and 3.2 msec. Intermediate conditions are present in the central part of the injection period ($\Delta t = 1.2, 1.6$ and 2.0 msec). The patterns relative to the high temperature environment are always smaller than the corresponding "cold" one, as it can be easily envisaged considering this shrinkage caused by pe-

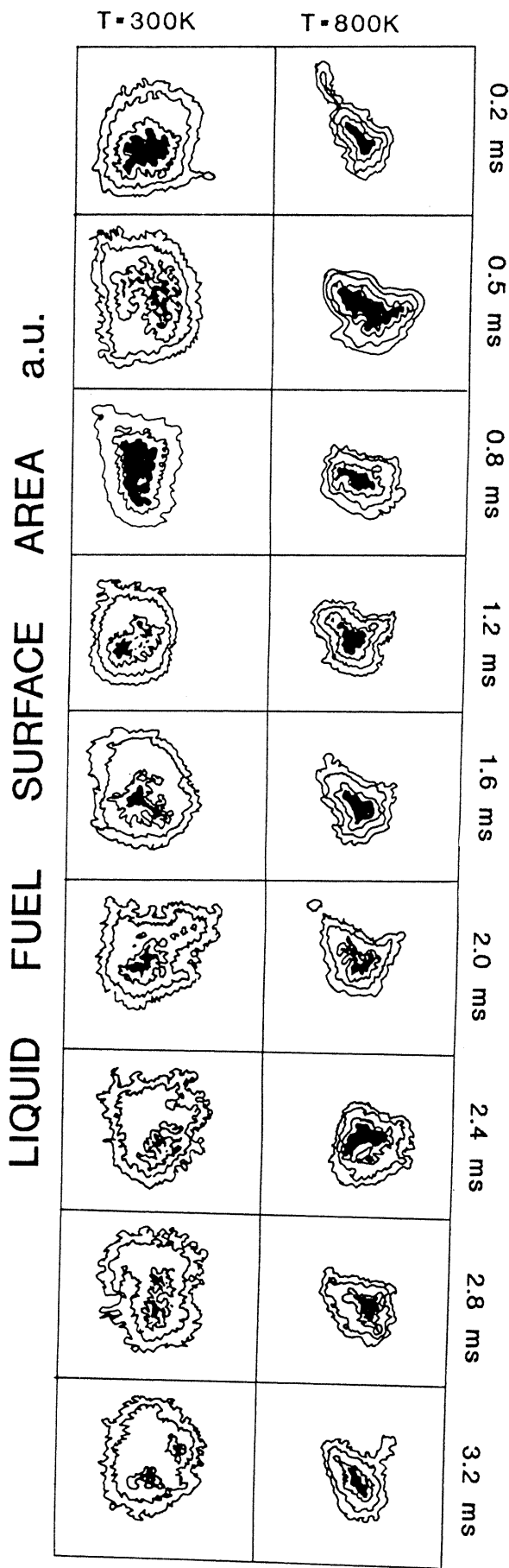


Figure 6 p = 15 bar
z = 14 mm

ripheral vaporization. The central part of the spray cross sections is also in this case covered by high values of the surface area, but it extends more widely respect to the previous conditions so that the outer annulus of decreasing values is narrowed. The only possible explanation of this effect is that the atomization is more effective in this condition; it can be conjectured that higher temperatures of the droplets reduce the surface tension and consequently the liquid skin is more prone to fragmentation. These qualitative comments in some cases can be expressed in more quantitative form, when a statistical descriptor can be used. For instance it was possible to elaborate the images in hot conditions, (those one reported in Fig. 6 are only a sample), with a four-step procedure .

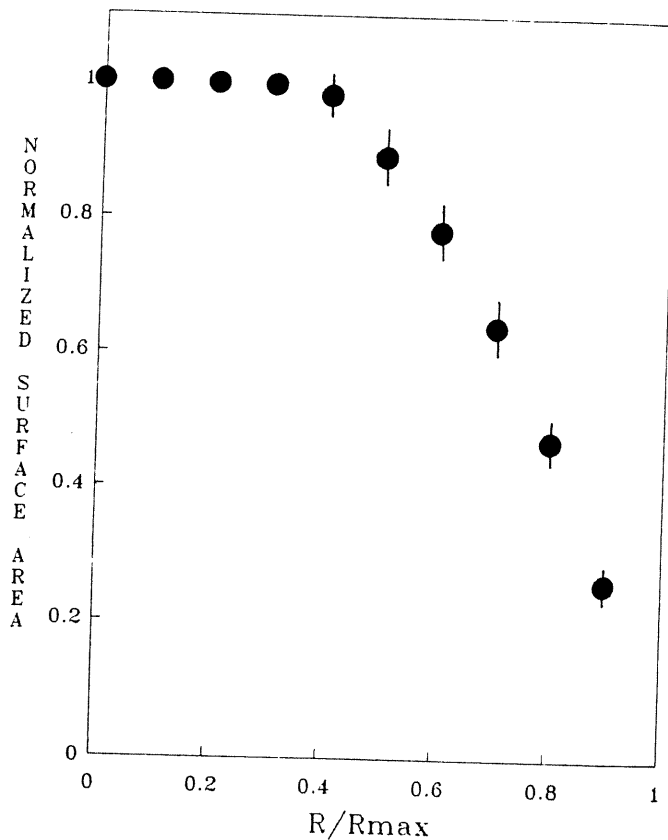


Figure 7

The first step was to compute the gravity center of each image, according to the formula:

$$x_G = \frac{\sum_{ij} x_{ij} I_{ij}}{\sum_{ij} I_{ij}}$$

For a fixed orthogonal coordinate system, x_G is the x coordinate of the gravity center, x_{ij} and I_{ij} are, respectively, the x coordinate of the pixel at i-th column and j-th row, and the intensity level in that pixel. Analogously it can be computed the coordinate y_G .

The second step was to sample the intensity levels along two perpendicular axes passing through the gravity center generating an ensemble of linear histograms with intensity, levels on the ordinate and the distance from the gravity center on abscissa. The third step consisted in normalizing all the histograms respect to the intensity value in the gravity center (the ordinate values) and the maximum distance from the gravity center (the abscissae values).

Finally the last step was to compute the average value of the intensities for each normalized radial position. The result of this procedure is shown in Fig. 7, in which the standard deviations are also reported as error bars.

The curve shows that the central part of the spray, which extends for a third of the cross section, is covered by statistically uniform high values, whereas the intensity level decrease monotonously in the outer part. It is also of interest to evidence that the error bars are narrower in the central part respect to those ones in the periphery and that the only uncorrelable values were recorded for r/r_{max} higher than 0.9, so that no average value was reported in the figure. The relevance of this type of statistical elaboration is immediate; it is not possible to compare results from numerical modelling with the experimental ones obtained with average on ensembles of samples taken at the same geometrical point, because the spray cross section changes in position and in dimensions.

FINAL REMARKS

The common feature of digital imaging makes many techniques, which use different characteristics of interaction of light with matter and different optical set-up, similar from the point of view of data elaboration.

Three different categories of numerical procedures can be used in this process. The first one can be defined image pre-processing and it deals with image enhancement procedures which reject the noise background of the images. The second one can be defined "image post-processing" and it deals with dedicate procedures specific for each process, which yield statistical elaboration or diagrams of morphological descriptors of image sequences.

Between these two categories there is the "image processing", which deals with different representations of a single image or of parts of an image. The paper has been focused on the methodological aspect of the first two categories of procedures and it has offered selected examples which should be of interest for researches in the field of diesel combustion.

REFERENCES

- 1) Azzarelli, L., Chimenti, , Salvetti, O., and Tognotti, L., "Image Processing in Spray Diagnostics: High Velocity Jets". Submitted to Atomization & Spray, (1989).
- 2) Cavaliere, A., Pintus, S., Tognotti, L., and Zanelli S., "Image Processing for the Analysis of Pre-ignition Mechanism in a Diesel Combustion Engine". Submitted to Atomization & Spray, (1989).
- 3) Fantini, E., Tonazzini, A., and Tognotti, L., "Drop Size Distribution in Sprays by Image Processing". Submitted to Comp. Chem. Engng., (1989).
- 4) Cavaliere, A., Ragucci, R., D'Alessio, A., and Noviello, C., Twenty-second Symp. (Int.) on Comb., p. 1973, The Combustion Institute, 1988.
- 5) Ragucci, R., Cavaliere, A., D'Alessio, A., "Laser Assisted Diagnostics for Characterization of Condensed Phases During Diesel Combustion Processes", COMODIA 90, Sept. 3-5, 1990, Kyoto, Japan.